ORIENTAL JOURNAL OF CHEMISTRY
An International Open Access, Peer Reviewed Research Journal
www.orientjchem.org
ISSN: 0970-020 X
CODEN: OJCHEG
2026, Vol. 42, No.(4):
Pg. 1302-1314

Performance Evaluation of Nano-SiO_2, Nano-Al_2O_3, and Nano-$CaCO_3$ Admixed Cementitious Composites

SURESH KUMAR VERMA[1], MD DANIYAL[2]* and DULAL GOLDAR[1]

[1]Department of Civil Engineering, Lingaya's Vidyapeeth, Faridabad, India
[2]Department of Civil Engineering, Sandip University, Madhubani, India
*Corresponding author E-mail: daniyalzhcet@gmail.com

http://dx.doi.org/10.13005/ojc/420406

(Received: October 09, 2025; Accepted: March 02, 2026)

ABSTRACT

This study evaluates the effects of Nano-SiO_2, Nano-Al_2O_3, and Nano-$CaCO_3$ on the fresh, mechanical, electrical, corrosion, and microstructural behavior of cementitious composites. A slight decrease in workability was observed in nano-silica mixes due to its high surface area, while nano-calcium carbonate improved mix cohesion. All nano-modified concretes exhibited higher compressive strength, with nano-silica providing the greatest improvement as a result of its strong pozzolanic reaction and ability to refine the microstructure. At a 3% replacement level, all three nanomaterials significantly enhanced overall performance. Durability assessments further showed higher electrical resistivity in nano-modified mixes, reflecting reduced ionic penetration. Corrosion studies using potentiodynamic polarization after 90 days of exposure indicated substantial improvements, especially under aggressive environments. Concrete incorporating nano-silica recorded the lowest corrosion current density and corrosion rate in tap water, saline water, and acidic solutions, followed by nano-alumina. These enhancements are primarily linked to microstructural densification, reduced permeability, and better stability of the passive layer formed on embedded steel reinforcement.

Key words: Nano-SiO_2; Nano-Al_2O_3; Nano-$CaCO_3$; Compressive strength; Electrical resistivity; Corrosion resistance.

INTRODUCTION

Concrete is one of the most commonly used construction materials due to its versatility, strength, and economic advantages. It forms the backbone of infrastructure such as buildings, bridges, and roadways worldwide. However, conventional concrete also has notable limitations. Its tensile capacity is relatively low, making it susceptible to cracking under tensile stresses. In addition, exposure to aggressive environments can degrade its performance, while corrosion of embedded steel reinforcement over time further compromises structural integrity. These factors lead

to cracking, durability loss, and a shortened service life, particularly in conditions involving chlorides, chemicals, or other harsh agents[1].

In recent years, nanotechnology has emerged as a transformative approach in material design and engineering. This field enables the development of extremely fine particles, known as nanomaterials, typically ranging from 1 to 100 nanometers in size. Owing to their extremely small dimensions, these materials exhibit distinctive physical and chemical properties that can be effectively harnessed to enhance the performance of construction materials[2].

Nanomaterials have demonstrated considerable promise in enhancing the properties of cement-based composites[3-5]. Among them, nano-silica effectively fills micro-voids within the cement matrix, accelerates hydration through the consumption of calcium hydroxide (CH), and promotes microstructural refinement, leading to improved mechanical performance and durability[6-10]. Nano-alumina aids in matrix densification and increases both compressive and flexural strength by acting as a nucleation promoter and micro-filler[11]. Likewise, nano-$CaCO_3$ functions as an efficient nucleating agent that accelerates cement hydration while contributing to strength development and pore structure refinement[12-14].

Nano-titanium dioxide is recognized for improving concrete durability while also providing self-cleaning and air-purifying functions through photocatalytic activity. Its effect on mechanical performance, however, is strongly dependent on dosage and mix composition, with reported outcomes varying across different formulations[15]. Among the various nanomaterials, carbon nanotubes (CNTs) stand out due to their outstanding reinforcing potential. Even at very low dosages, CNTs can markedly enhance both compressive and tensile strength, while simultaneously reducing shrinkage, porosity, and chloride ingress. In addition, CNTs introduce functional attributes such as electrical conductivity, allowing the development of self-sensing concrete systems; nevertheless, achieving uniform dispersion of CNTs within the cement matrix remains a significant technical challenge[16].

Despite the advancements achieved so far, direct comparative studies evaluating nano-SiO_2, nano-Al_2O_3, and nano-$CaCO_3$ under identical experimental conditions remain limited. Furthermore, the long-term performance of concrete incorporating these nanomaterials when exposed to aggressive environments has not been sufficiently explored, and clear recommendations regarding their optimum dosage levels are still lacking.

In response to these gaps, the present study undertakes a systematic comparison of nano-SiO_2 (NS), nano-Al_2O_3 (NA), and nano-$CaCO_3$ (NC) with respect to their influence on the fresh properties, mechanical performance, corrosion resistance, and microstructural features of concrete. The outcomes of this research are expected to support the development of durable, high-performance concrete mixes suitable for use in demanding and critical infrastructure applications.

MATERIAL AND METHODS

Cement

This study utilized Ordinary Portland Cement (OPC) of 43 grade as the primary binding material in all concrete mixtures. The cement exhibits an average particle size of approximately 20 µm and a fineness value of 5.6%, which is well below the maximum limit of 10% specified in IS 4031 (Part 1):1988. The normal consistency of the cement was measured as 33%, indicating an appropriate and stable water demand for hydration. The initial and final setting times were found to be 68 minutes and 390 minutes, respectively, both of which comply with the requirements of IS 4031 (Part 5):1988, which prescribe a minimum initial setting time of 30 minutes and a maximum final setting time of 600 minutes. Regarding strength development, the cement attained compressive strengths of 23.3 MPa at 3 days, 33.4 MPa at 7 days, and 43.7 MPa at 28 days, satisfying the strength criteria specified for 43-grade OPC in IS 4031 (Part 6):1988.

The microstructural features and elemental composition of the cement were characterized using Scanning Electron Microscopy (SEM) and Energy-Dispersive X-ray Spectroscopy (EDX), respectively. The SEM images presented in Fig. 1 show that the OPC particles exhibit irregular, angular, and rough surface textures, indicating a heterogeneous morphology. Such particle characteristics suggest

comparatively loose packing, which may contribute to the presence of voids within the cementitious matrix.

EDX analysis confirms the chemical suitability of the cement for durable concrete production. The composition is dominated by oxygen (47.18%) and calcium (36.11%), which are essential for the formation of calcium silicate hydrate (C–S–H) during hydration. Other significant elements include silicon (7.19%), aluminium (2.78%), and iron (2.88%), which participate in the formation of key clinker phases such as C_3S, C_2S, C_3A, and C_4AF. Sulphur (1.46%), mainly derived from gypsum, plays a vital role in regulating setting time, while potassium (1.27%) and magnesium (1.13%) are present within permissible limits, ensuring dimensional stability and minimizing the risk of adverse chemical reactions.

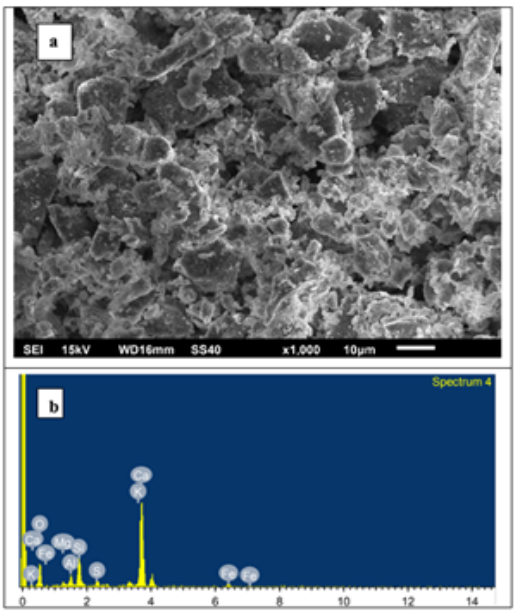

Fig. 1: (a) SEM micrograph (b) EDX Spectrum of OPC Aggregate

Locally available crushed quartzite was used as the coarse aggregate (CA), having a fineness modulus of 2.65, while the fine aggregate (FA) comprised locally sourced coarse sand with a fineness modulus of 3.27. These aggregates were selected based on their availability and proven suitability for structural concrete applications.

To determine the particle size distribution, sieve analysis was carried out in accordance with IS: 383 for both coarse and fine aggregates, and the results are presented in Fig. 2 and Fig. 3, respectively. Aggregate grading plays a crucial role in governing the performance of concrete in both fresh and hardened conditions. An appropriate gradation promotes efficient particle packing, minimizes voids, and helps achieve an optimal water–cement ratio, thereby enhancing the mechanical strength and long-term durability of the concrete mix.

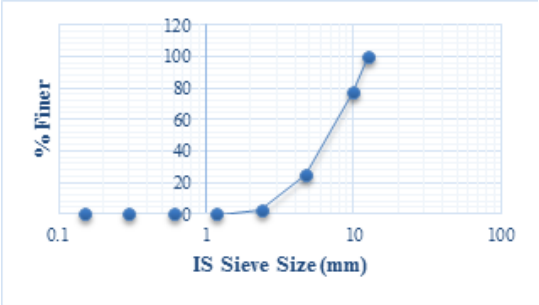

Fig. 2: Particle size distribution curve of CA

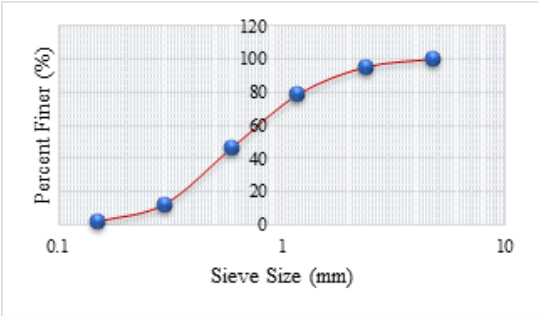

Fig. 3: Particle size distribution curve of FA

Nanomaterials

The investigation incorporated three different nanomaterials—nano-silica (NS), nano-alumina (NA), and nano-calcium carbonate (NC), each having a purity exceeding 99%. The nano-silica particles possessed an average size of approximately 20 nm and a high specific surface area of about 500 m^2/g, whereas nano-alumina and nano-calcium carbonate exhibited mean particle sizes close to 30 nm with specific surface areas of roughly 450 m^2/g.

The morphological features and elemental composition of the nanomaterials were characterized using Scanning Electron Microscopy (SEM) and

Energy Dispersive X-ray (EDX) analysis. These techniques are effective in assessing particle shape, surface characteristics, and compositional purity. The SEM micrographs presented in Fig. 4(a), Fig. 5(a), and Fig. 6(a) show the surface morphology of NS, NA, and NC, respectively. Nano-silica is observed as ultra-fine, nearly spherical particles with noticeable agglomeration, a common feature of materials with very high surface area. Nano-alumina displays irregular yet relatively compact particle shapes, while nano-calcium carbonate exhibits more distinct crystalline or rod-like morphologies.

The corresponding EDX spectra shown in Fig. 4(b), Fig. 5(b), and Fig. 6(b) verify the elemental composition of the nanomaterials. Prominent peaks confirm the dominance of silicon and oxygen in nano-SiO_2, aluminium and oxygen in nano-Al_2O_3, and calcium, carbon, and oxygen in nano-$CaCO_3$. These observations validate the high purity and structural suitability of the selected nanomaterials for enhancing the microstructure and performance of cementitious composites.

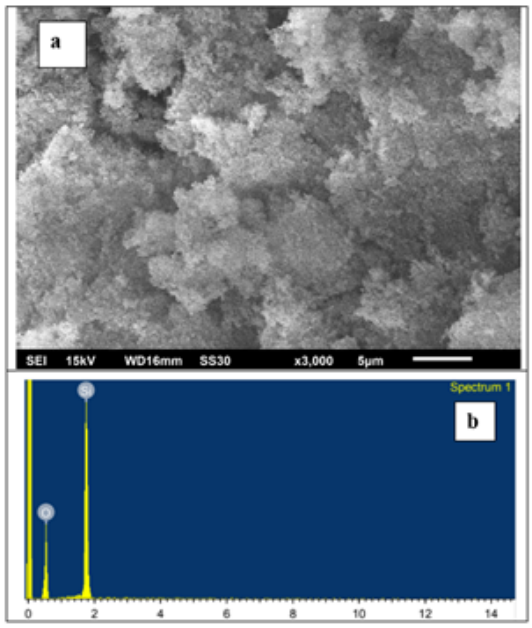

Fig. 4: (a) SEM micrograph (b) EDX spectra of NS

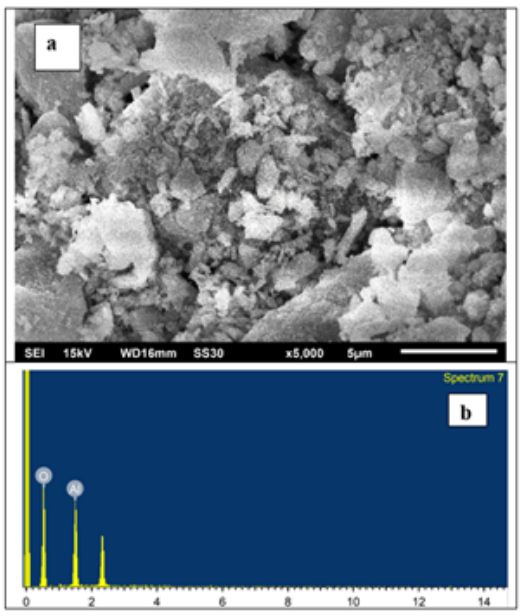

Fig. 5: (a) SEM micrograph (b) EDX spectra of NA

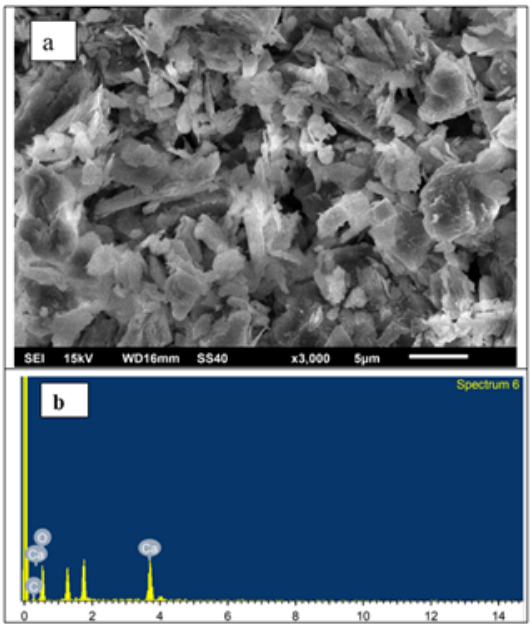

Fig. 6: (a) SEM micrograph (b) EDX spectra of NC

Exposure Environments

The concrete samples in this research were subjected to three distinct exposure environments to assess their durability under varying conditions. These environments were chosen to replicate typical field situations encountered in civil engineering structures.

Tap water with a pH of 7.11 was used to represent normal exposure conditions found in

freshwater or routine construction settings. This served as the control environment for comparing the inherent performance of the concrete mixes without any chemically aggressive influence. A 3.5% NaCl saline solution with a pH of 7.27 was employed to imitate marine or coastal environments where elevated chloride levels can accelerate the corrosion of steel reinforcement. An acidic solution made by adding 1% H_2SO_2, having a pH of 1.12, was used to simulate severe industrial or chemical exposure conditions, such as those encountered in wastewater systems or areas adjacent to chemical industries.

Mix Proportions

Table 1 outlines the complete mix proportions adopted in this study, where nano-materials were incorporated by partially replacing cement at levels of 1%, 3%, and 5% (by weight). The concrete mixes were prepared using a proportion of 1:1.5:3 for OPC, fine aggregates, and coarse aggregates, with the water–cement ratio kept constant at 0.5.

In total, ten different mix combinations were developed to analyse how nano-alumina (NA), nano-silica (NS), and nano-calcium carbonate (NC) influence concrete behaviour. The reference mix without any nano-additive served as the control, while the remaining mixes included 1%, 3%, and 5% cement replacement using each nanoparticle type. This systematic approach allowed for a clear and direct comparison of the effects of the various nano-materials on concrete performance.

Specimen specifications and Test procedures

Workability of the concrete mixes incorporating nanomaterials as partial cement replacements was evaluated through the slump test, using the standard slump cone apparatus, which consists of a hollow frustum-shaped cone. The procedure followed the guidelines of IS 1199:1959 to determine the consistency and ease of flow of the fresh concrete.

For compressive strength assessment, a total of twelve cubes of 150 mm size were cast for each mix. After 24 hours, the specimens were demoulded and transferred to a curing tank filled with potable water, where they were kept for 28 days. At the end of the curing period, compressive strength tests were performed on three cubes from every mix to determine the 28-day compressive strength.

The remaining nine cubes from each mix were grouped into three sets and subjected to different exposure conditions: tap water, saline water containing 3.5% NaCl, and an acidic solution with 1% H_2SO_4. These specimens were stored in their respective environments for a total period of 90 days. To ensure uniform exposure throughout the study, all solutions were replaced every two weeks, maintaining stable pH values and ionic concentrations.

Before testing, each specimen was rinsed with tap water to remove any surface residues or loose particles. Compressive strength was measured using a 1000 kN capacity compression testing

Table 1. Mix Proportions of Concrete

Mix Variant	Cement (kg/m^3)	Nano Additive (kg/m^3)	FA (kg/m^3)	CA (kg/m^3)	Water (kg/m^3)
Control (X0)	382.00	0.00	573.00	1146.00	191.00
1% nano-Al_2O_3 (NA1)	378.18	3.82	573.00	1146.00	191.00
3% nano- Al_2O_3 (NA3)	370.54	11.46	573.00	1146.00	191.00
5% nano- $Al2O_3$ (NA5)	362.90	19.10	573.00	1146.00	191.00
1% nano-SiO_2 (NS1)	378.18	3.82	573.00	1146.00	191.00
3% nano-SiO_2 (NS3)	370.54	11.46	573.00	1146.00	191.00
5% nano-SiO_2 (NS5)	362.90	19.10	573.00	1146.00	191.00
1% nano-$CaCO_3$ (NC1)	378.18	3.82	573.00	1146.00	191.00
3% nano- $CaCO_3$ (NC3)	370.54	11.46	573.00	1146.00	191.00
5% nano-$CaCO_3$ (NC5)	362.90	19.10	573.00	1146.00	191.00

machine (AIMIL Ltd., least count 1 kN), applying a steady, uniform load until failure occurred. For every exposure condition, the compressive strength value was obtained by averaging the results of three specimens, and these values were used for subsequent analysis.

To examine the influence of nanomaterials on electrical resistivity, cylindrical concrete specimens measuring 150 × 300 mm were cast. After demoulding, all cylinders were cured in tap water for 28 days. Following the curing period, the specimens were placed under different environmental exposure conditions for an additional 90 days. Electrical resistivity was then measured using a Proceq Resipod device to assess the durability characteristics of nano-enhanced concrete subjected to varied exposure environments.

The corrosion behaviour of embedded steel reinforcement was evaluated using the Tafel potentiodynamic polarization method. For each mix type, nine cylindrical specimens with dimensions of 100 mm in diameter and 200 mm in height were prepared, each containing a centrally positioned steel bar. To maintain a consistent concrete cover of 45 mm on the sides and bottom, the steel rod was arranged so that it extended 30 mm above the mould surface, as shown in Fig. 7. The portion of the bar protruding above the concrete surface was initially wrapped with insulating tape, which was removed before testing to allow electrical connections. Corrosion kinetics and corrosion rate (CR) were measured using an ACM corrosion monitoring instrument.

SEM analysis was carried out to examine the microstructural features of the hardened concrete specimens. After 28 days of curing, small portions of the concrete were extracted and thoroughly dried to remove any residual moisture. These fragments were trimmed into pieces approximately 10 mm in size, affixed to SEM stubs using conductive adhesive, and subsequently coated with a thin layer of gold or carbon to ensure proper electrical conductivity.

The prepared samples were then placed in the SEM chamber, where a focused electron beam scanned their surfaces to produce high-resolution images. The resulting micrographs provided insights into hydration products, pore distribution, microcracks, and the interaction between the cement paste, aggregates, and incorporated nanoparticles. This analysis facilitated a deeper understanding of the densification, morphological changes, and overall microstructural enhancements achieved in nano-modified concrete relative to the control mix.

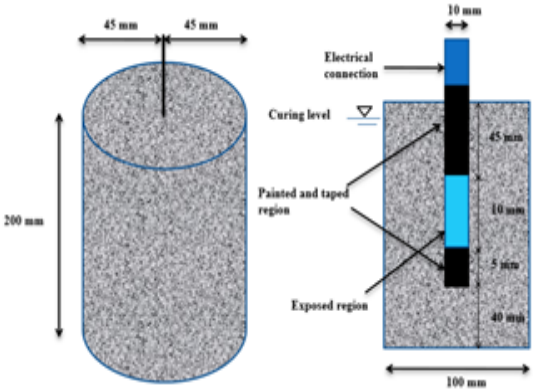

Fig. 7: Schematic diagram of specimen for corrosion test

RESULTS AND DISCUSSION

Workability

Workability of the fresh concrete mixes containing different types and dosages of nanomaterials was evaluated using the slump test, and the results are illustrated in Fig. 8. The reference mix without nano-additives (X0) exhibited a slump value of 75 mm, corresponding to medium workability. The introduction of nano-alumina resulted in a progressive reduction in slump with increasing replacement levels. Specifically, slump values decreased to 70 mm at 1% replacement (NA1), 60 mm at 3% (NA3), and 50 mm at 5% (NA5), indicating a transition from medium to low workability as the nano-alumina content increased.

A comparable reduction trend was observed for mixes incorporating nano-silica. Slump values declined from 68 mm for NS1 to 55 mm for NS3 and further to 45 mm for NS5, reflecting a shift from medium to distinctly low workability. In contrast, concrete mixes containing nano-calcium carbonate experienced a relatively smaller reduction in slump. The measured values were 72 mm for NC1, 60 mm for NC3, and 52 mm for NC5, demonstrating that nano-$CaCO_3$ had a less pronounced effect on flowability at similar replacement levels.

The observed decrease in workability with increasing nano-material dosage can be attributed to the extremely fine particle size and high specific surface area of nanomaterials, which significantly increase water demand. Among the three additives, nano-silica exhibited the greatest reduction in slump, likely due to its higher surface area and greater chemical reactivity. Conversely, nano-calcium carbonate caused the least decline in workability, suggesting a comparatively lower impact on the rheological behaviour of the fresh mix.

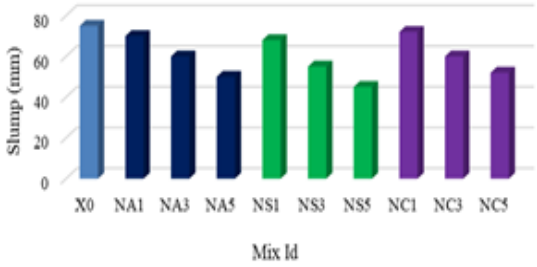

Fig. 8: Effect of nano-additive on workability of concrete

Compressive Strength

The 28-day compressive strength results presented in Fig. 9 indicate that the inclusion of nano-additives consistently improves strength relative to the control mix (X0: 28.5 MPa), although the extent of improvement strongly depends on the type and dosage of the nano-material. At a 1% replacement level, both nano-alumina (NA1) and nano-silica (NS1) produced moderate strength enhancements of 12.3% and 9.5%, respectively. A more pronounced improvement was observed at the 3% replacement level, where NA3 and NS3 achieved peak strength gains of 24.6% and 26.3%, corresponding to compressive strengths of 35.5 MPa and 36.0 MPa. Increasing the replacement level to 5% (NA5 and NS5) resulted in a reduction in strength compared to the optimum 3% dosage, although the values remained higher than that of the control mix, reaching 33.8 MPa for nano-alumina and 34.0 MPa for nano-silica. In contrast, nano-calcium carbonate exhibited a comparatively modest influence on compressive strength development. The maximum improvement for this additive occurred at 3% replacement (NC3), yielding a 12.3% increase and a strength of 32.0 MPa. Lower and higher dosages (1% and 5%) resulted in smaller gains of 3.5% and 10.5%, respectively, confirming the limited but beneficial role of nano-$CaCO_3$.

The observed trends can be attributed to the combined effects of particle filling, nucleation enhancement, and pozzolanic reactivity, depending on the nano-material. Nano-silica, with its high surface area and strong pozzolanic nature, reacts with calcium hydroxide to form additional C–S–H gel, leading to matrix densification and pore refinement, particularly at the optimal 3% dosage. Nano-alumina primarily acts as a nucleation promoter and micro-filler, accelerating hydration and improving particle packing; however, excessive content beyond the optimal level may cause agglomeration and hinder uniform dispersion. Nano-calcium carbonate mainly contributes through filler and seeding mechanisms, promoting early hydration but exhibiting limited chemical reactivity, which explains the comparatively lower strength gains. The decline in performance at 5% replacement across all nano-additives is likely associated with particle agglomeration, reduced workability, the formation of micro-voids, and partial dilution of the cementitious matrix, all of which adversely affect hydration efficiency and strength development.

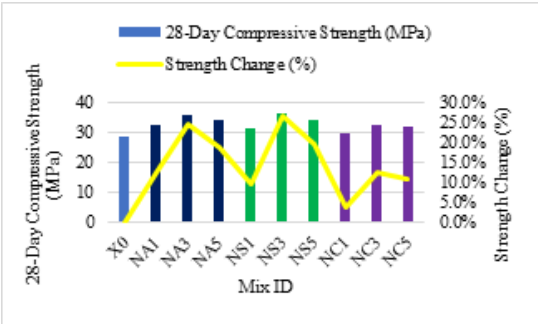

Fig. 9: Impact of nano-additive on 28-days Compressive Strength

The compressive strength performance of concrete mixes incorporating nano-admixtures after 90 days of exposure to different environments is presented in Fig. 10. The results indicate a clear improvement in strength retention and durability for nano-modified concretes compared with the control mix (X0), particularly under aggressive exposure conditions.

The control mix (X0) achieved a compressive strength of 31 MPa under tap water

curing. However, exposure to saline and acidic environments resulted in a reduction to 29.5 MPa and 27.2 MPa, respectively, highlighting the susceptibility of conventional concrete to chemical attack and strength degradation.

Concrete mixes containing nano-alumina (NA) exhibited a significant enhancement in compressive strength across all environments. At 1% replacement (NA1), strengths increased to 34.2 MPa in tap water, 32.2 MPa in saline water, and 30.4 MPa in acidic water. The maximum improvement was observed at 3% nano-alumina (NA3), where compressive strengths of 38.1 MPa, 36 MPa, and 34 MPa were recorded under tap, saline, and acidic conditions, respectively. Although the 5% replacement level (NA5) maintained higher strength than the control mix, a slight reduction compared to NA3 suggests that excessive nano-alumina may reduce dispersion efficiency.

The incorporation of nano-silica (NS) resulted in the most pronounced strength enhancement among all nano-materials. The NS1 mix achieved compressive strengths of 33.5 MPa, 31.2 MPa, and 29 MPa in tap, saline, and acidic environments, respectively. The optimum performance was attained at 3% nano-silica (NS3), which exhibited the highest compressive strengths of 39 MPa in tap water, 37.2 MPa in saline water, and 35.2 MPa in acidic water. Even at a higher dosage (NS5), the compressive strength remained superior to the control, although marginally lower than NS3.

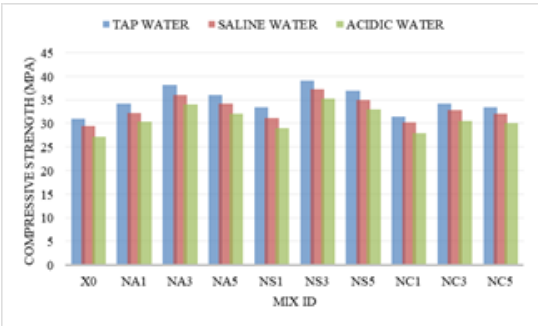

Fig. 10: Compressive strength of concrete under different exposure conditions after 90 days

Concrete mixes modified with nano-calcium carbonate (NC) also demonstrated improved compressive strength relative to X0, though the enhancement was less pronounced than that achieved with nano-alumina and nano-silica. At 1% replacement (NC1), compressive strengths of 31.5 MPa, 30.2 MPa, and 28 MPa were recorded in tap, saline, and acidic environments, respectively. The best performance for nano-calcium carbonate was observed at 3% (NC3), yielding strengths of 34.2 MPa, 32.8 MPa, and 30.5 MPa, followed by a slight reduction at 5% replacement (NC5).

Electrical resistivity

Electrical resistivity is a key indicator of concrete durability, as higher resistivity corresponds to reduced ionic transport and improved protection of embedded steel against corrosion. Figure 11 presents the electrical resistivity values of the control and nano-modified concrete mixes after 90 days of exposure to tap water, saline water, and acidic water. The results clearly demonstrate the influence of nano-admixtures and their dosage on the resistivity performance of concrete.

The control mix exhibited the lowest resistivity values in all exposure conditions, recording 19.8 kΩ·cm in tap water, 17.4 kΩ·cm in saline water, and 14.8 kΩ·cm in acidic water. The progressive reduction in resistivity from tap water to acidic environments reflects increased ionic conductivity and greater vulnerability of conventional concrete under aggressive conditions.

The incorporation of nano-alumina (NA) resulted in a notable enhancement in electrical resistivity across all environments. At 1% replacement (NA1), resistivity increased moderately to 21.1, 19.1, and 16.5 kΩ·cm in tap, saline, and acidic media, respectively. The maximum improvement was observed at 3% nano-alumina (NA3), where resistivity values reached 25.9 kΩ·cm in tap water, 21.3 kΩ·cm in saline water, and 18.2 kΩ·cm in acidic water. A slight reduction was observed at 5% replacement (NA5), suggesting that excessive nano-alumina may lead to particle agglomeration and reduced efficiency, despite still outperforming the control mix.

Among all nano-admixtures, nano-silica (NS) produced the most pronounced improvement in electrical resistivity. At 1% dosage (NS1), resistivity values increased to 24.2, 20.2, and 17.6 kΩ·cm in tap, saline, and acidic environments, respectively.

The highest resistivity values were achieved with 3% nano-silica (NS3), recording 28.6 kΩ·cm in tap water, 24.0 kΩ·cm in saline water, and 21.2 kΩ·cm in acidic water. These results indicate superior resistance to ionic penetration, attributed to the high pozzolanic reactivity of nano-silica and its strong pore-refining effect. Although the resistivity remained high at 5% replacement (NS5), a marginal decline compared to NS3 was noted, again indicating reduced dispersion efficiency at higher dosages.

The addition of nano-calcium carbonate (NC) also improved resistivity compared to the control mix, though to a lesser extent than nano-alumina and nano-silica. At 1% replacement (NC1), resistivity values increased slightly to 21.1, 18.2, and 15.5 kΩ·cm. The optimum performance for nano-calcium carbonate was observed at 3% (NC3), with values of 23.0 kΩ·cm in tap water, 19.6 kΩ·cm in saline water, and 16.9 kΩ·cm in acidic water. A further increase to 5% (NC5) resulted in a minor reduction in resistivity, reflecting the limited pozzolanic activity of nano-$CaCO_2$ compared to nano-alumina and nano-silica.

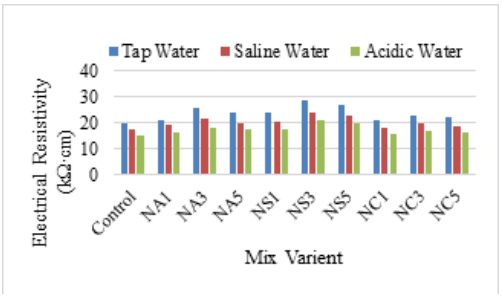

Fig. 11: Electrical resistivity of concrete under different exposure conditions after 90 days

Corrosion Behaviour

The potentiodynamic Tafel polarization responses of bare steel, control concrete, and nano-modified concrete specimens (NS3, NA3, and NC3) after 90 days of exposure to tap water, saline water, and acidic media are illustrated in Fig. 12, Fig. 13, and Fig. 14, respectively. The polarization curves were analyzed to extract key electrochemical corrosion parameters, including the anodic Tafel slope ($_2$a), cathodic Tafel slope ($_2$c), corrosion potential (Ecorr), corrosion current density (Icorr), and corrosion rate (CR). A detailed summary of the calculated corrosion characteristics for all exposure conditions is provided in Table 2.

The electrochemical characteristics obtained from the Tafel polarization analysis clearly demonstrate substantial variations in the corrosion behaviour of bare steel, control concrete, and nano-modified concrete specimens (NC3, NA3, and NS3) across different exposure environments. The results confirm the effectiveness of nano-additives in enhancing the corrosion resistance of embedded steel reinforcement.

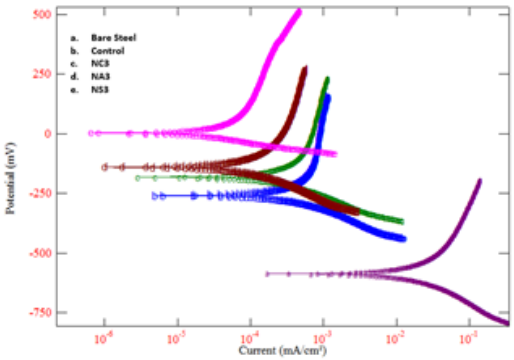

Fig. 12: Tafel plots of samples immersed in tap water

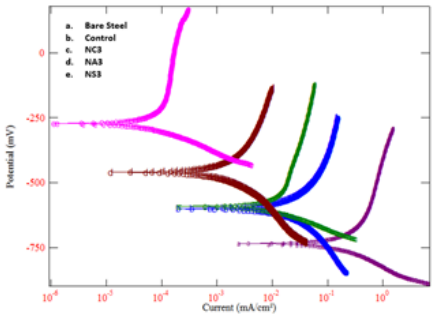

Fig. 13: Tafel plots of samples immersed in saline water

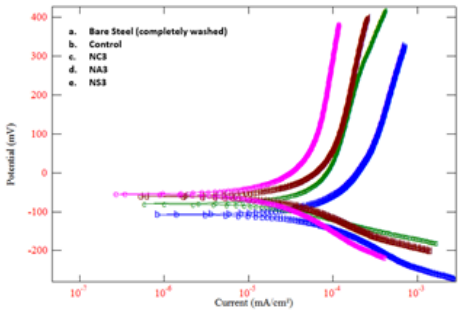

Fig. 14: Tafel plots of samples immersed in acidic water

Table 2: Kinetic characteristics of steel corrosion in various exposure media

Exposure media	Specimen Name	βa (mV)	βc (mV)	Ecorr (mV)	Icorr (mA/cm²)	Corrosion Rate (mm/yr)
Tap Water	Bare Steel	989.62	150.91	-378.75	0.015745	0.1824895
	Control	1568.1	179.53	-258.54	0.000544	0.0063012
	NC3	1168.7	135.47	-179.34	0.000336	0.0038965
	NA3	990.19	132.96	-28.897	0.00012	0.0013906
	NS3	487.88	65.782	1.7745	0.0000164	0.0001898
Saline Water	Bare Steel	720.33	94.245	-734.42	0.1460066	1.6922
	Control	600.2	237.2	-599.5	0.0414599	0.4805205
	NC3	864.23	98.845	-590.92	0.0065635	0.0760707
	NA3	478.26	230.7	-461.97	0.0033549	0.0388836
	NS3	675.05	141.41	-274.99	0.00009	0.0010436
Acidic Water	Control	729.43	139.71	-106.94	0.0000954	0.0011057
	NC3	562.88	101.56	-83.572	0.00002463	0.0002855
	NA3	985.72	68.051	-61.073	0.00001906	0.0002209
	NS3	1231.8	85.822	-56.854	0.00001469	0.0001703

Under tap water exposure, bare steel exhibited the poorest performance, characterized by the highest corrosion current density (0.0157 mA/cm²) and corrosion rate (0.1825 mm/yr), indicating its high vulnerability in the absence of any protective matrix. Incorporation of conventional concrete significantly reduced the corrosion rate to 0.0063 mm/yr, highlighting the inherent shielding effect of the cementitious system. Further improvement was achieved with nano-modified mixes. Among them, NS3 showed superior electrochemical stability, recording the lowest corrosion current density ($1.64 \times 10_{22}$ mA/cm²) and corrosion rate (0.00019 mm/yr), followed by NA3 (0.00139 mm/yr) and NC3 (0.00390 mm/yr). The pronounced reduction in corrosion parameters for NS3 confirms the beneficial role of nanosilica in refining the microstructure and strengthening the passive film in neutral environments.

Exposure to saline water resulted in a marked increase in corrosion activity due to the aggressive action of chloride ions. Bare steel experienced severe degradation, as evidenced by a high corrosion current density of 0.1460 mA/cm² and corrosion rate of 1.6922 mm/yr. Although the control concrete reduced the corrosion rate to 0.4805 mm/yr, the nano-modified concretes provided substantially improved protection. The corrosion rates were further lowered to 0.0761 mm/yr for NC3 and 0.0389 mm/yr for NA3. Notably, NS3 exhibited exceptional resistance, with an extremely low corrosion rate of 0.00104 mm/yr. The significant positive shift in corrosion potential toward less negative values (–274.99 mV) for NS3 indicates enhanced passivation and effective suppression of chloride-induced corrosion processes.

In the acidic environment, all concrete mixes displayed comparatively lower corrosion rates than those observed under saline exposure, suggesting partial surface passivation in acidic media. The control specimen showed a corrosion rate of 0.00111 mm/yr, while NC3 and NA3 further improved corrosion resistance with rates of 0.00029 mm/yr and 0.00022 mm/yr, respectively. Once again, NS3 demonstrated the highest corrosion resistance, presenting the lowest corrosion current density ($1.47 \times 10_{22}$ mA/cm²) and corrosion rate (0.00017 mm/yr). The relatively noble corrosion potential (–56.85 mV) associated with NS3 reflects reduced electrochemical activity and enhanced protective behaviour under acidic conditions.

Microstructural Characteristics

The microstructural characteristics of the Control, NC3, NA3, and NS3 concrete mixes were examined using Scanning Electron Microscopy (SEM) after 28 days of curing to elucidate the influence of nanomaterials on hydration behavior, pore refinement, and matrix densification, as illustrated in Fig. 15 through Fig. 18.

SEM observations of the control mix indicate a non-uniform and relatively porous microstructure, marked by visible voids, microcracks, and loosely arranged C–S–H gel. Prominent calcium hydroxide (CH) crystals and partially hydrated cement particles are evident, suggesting incomplete hydration. Such features contribute to reduced durability and facilitate the ingress of aggressive species, thereby increasing the corrosion risk of embedded steel.

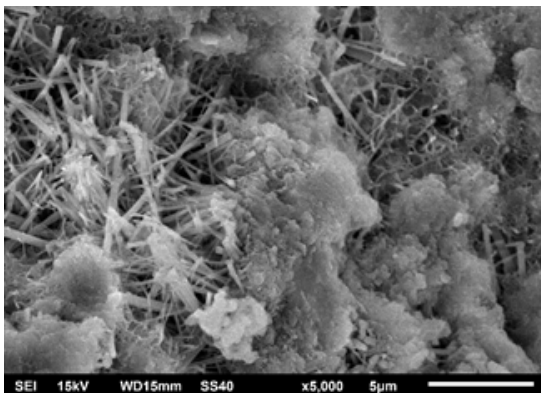

Fig. 15: SEM image of Control specimen

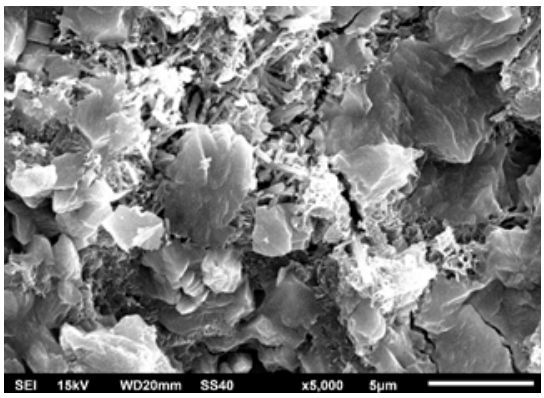

Fig. 16: SEM image of NC3 specimen

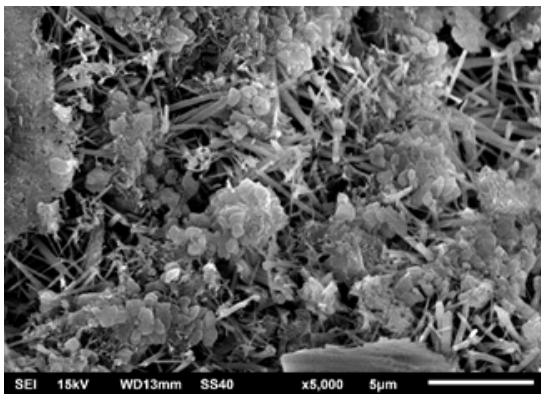

Fig. 17: SEM image of NA3 specimen

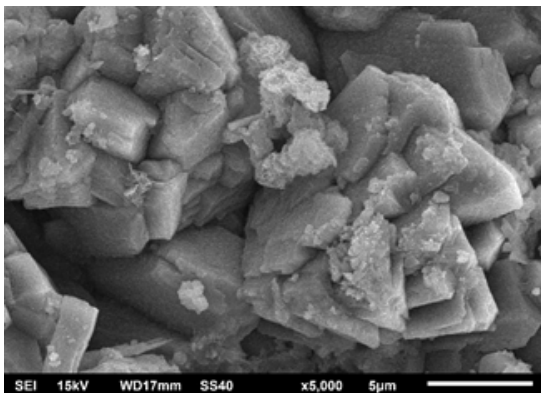

Fig. 18: SEM image of NS3 specimen

In comparison, the NC3 mix demonstrates a noticeably denser microstructure than the control specimen. The inclusion of nano-calcium carbonate promotes nucleation and accelerates cement hydration, resulting in improved C–S–H formation. Nevertheless, isolated micro-voids and occasional needle-shaped ettringite crystals are still observed, indicating that while pore refinement is achieved, the enhancement remains moderate relative to other nano-modified systems.

The NA3 mix exhibits substantial improvement in matrix compactness and uniformity. The presence of nano-alumina enhances pozzolanic activity, leading to the generation of additional C–S–H gel and a marked reduction in CH crystal size and quantity. SEM images reveal a more continuous microstructure with reduced pore interconnectivity and a well-developed interfacial transition zone (ITZ), which contributes to enhanced mechanical performance and increased resistance to chloride penetration.

Among all mixes, the NS3 specimen presents the most compact and homogeneous microstructure. Nano-silica actively participates in

pozzolanic reactions with CH, forming secondary C–S–H gel and substantially minimizing the presence of large CH crystals. The SEM micrographs reveal a densely packed matrix with minimal voids or microcracking, along with a significantly strengthened ITZ due to both filler and chemical effects of nano-silica. This refined microstructure directly correlates with the observed improvements in durability, electrical resistivity, and corrosion resistance reported in the electrochemical studies.

CONCLUSION

This study confirms that replacing cement with 3% (by weight) of Nano-SiO_2, Nano-Al_2O_3, or Nano-$CaCO_3$ leads to notable improvements in both the mechanical properties and durability of cementitious composites. Among the three, nano-silica exhibits the most pronounced effect because of its strong pozzolanic activity. It readily reacts with calcium hydroxide (CH) released during cement hydration to form additional calcium silicate hydrate (C–S–H) gel, which results in a denser microstructure, reduced porosity, higher strength, and improved corrosion resistance.

Nano-alumina enhances performance primarily through the formation of extra aluminate hydrates, which increases matrix cohesion and refines the internal structure. Nano-calcium carbonate functions mainly as a micro-filler and nucleation site, promoting early hydration and more uniform C–S–H development. Collectively, these nanomaterials lower permeability, limit microcrack formation, and support better passivation of embedded steel, thereby enhancing durability under harsh environments such as chloride-rich or sulphate-contaminated conditions.

The synergy between the nanoparticles and the hydration products not only provides early-age strength benefits but also contributes to long-term structural stability. As a result, nano-modified concrete emerges as a sustainable, high-performance option for modern construction, offering superior mechanical performance along with enhanced resistance to environmental deterioration.

ACKNOWLEDGEMENTS

The authors express their sincere gratitude to Lingaya's Vidyapeeth for overall support and to Aligarh Muslim University for providing access to SEM-EDX facilities.

Authors' Contributions

Suresh Kumar Verma conducted the experiments, data collection, and analysis. Md Daniyal and Dulal Goldar provided supervision, guidance, and critical revision of the manuscript.

Conflicts of Interest

The authors declare that they have no known financial or personal conflicts of interest in this study.

Funding Statement

This research did not receive any specific grant from funding agencies.

Data Availability Statement

The datasets generated and analysed during the current study are available from the corresponding author on reasonable request.

Ethical Approval Statement

This study did not involve human participants or animals; hence, formal ethical approval was not required.

Informed Consent Statement

Not applicable for this study as no human subjects were involved.

REFERENCES

1. AFïtcin, P. C., Cements of yesterday and today: Concrete of tomorrow., *Cement and Concrete Research*, **2000**, 30(9), 1349–1359.
2. Goel, G.; Sachdeva, P.; Chaudhary, A. K.; Singh, Y., The use of nanomaterials in concrete: A review., *Materials Today: Proceedings*, **2022,** 69(2), 365–371.
3. Safiuddin, M.; Gonzalez, M.; Cao, J.; Tighe, S. L., State-of-the-art report on use of nano-materials in concrete., *International Journal of Pavement Engineering*, **2014**, 15(10), 940–949.

4. Daniyal, M.; Azam, A.; Akhtar, S., Application of Nanomaterials in Civil Engineering., in *Nanomaterials and Their Applications*, Khan, Z. (Ed.), Springer, Singapore, **2018**, Vol. 84, 177–198.
5. Sujitha, V. S.; Ramesh, B.; Joseph Raj, X., Investigation of functionalized graphene oxide incorporated superabsorbent polymers for enhanced durability, hydration, microstructure and mechanical strength of modified concrete., *Composite Interfaces*, **2025**, 32(2), 177-214.
6. Al-Rifaie, W.; Alawaneh, A.; Al-Bajawi, M.; Ahmed, W., Effect of Nano Silica on Compressive Strength of Concrete., *Proceedings of ASME International Mechanical Engineering Congress and Exposition*, Pittsburgh, USA, **2018**, Vol. 12, V012T11A044.
7. Arif, M.; Hasan, S. D.; Siddiqui, S., Effect of nano silica on strength and permeability of concrete., *Materials Today: Proceedings*, **2023**.
8. Mahdikhani, M.; Bamshad, O.; Shirvani, M. F., Mechanical properties and durability of concrete specimens containing nano silica in sulfuric acid rain condition., *Construction and Building Materials*, **2018**, 167, 929–935.
9. Rupasinghe, M.; Mendis, P.; Ngo, T.; Nguyen, T. N.; Sofi, M., Compressive strength prediction of nano-silica incorporated cement systems based on a multiscale approach., *Materials and Design*, **2017**, 115, 379–392.
10. Nisar, N.; Rahman, I.; Paruthi, S.; Khan, A. H.; Sabi, E.; Alyaseen, A., Enhancing concrete properties with nano-SiO_2 and nano-TiO_2: a review., *Journal of Structural Integrity and Maintenance*, **2025**, 10(2).
11. Zhou, J.; Zheng, K.; Liu, Z.; He, F., Chemical effect of nano-alumina on early-age hydration of Portland cement., *Cement and Concrete Research*, **2019**, 116, 159–167.
12. Sun, Y.; Zhang, P.; Guo, W.; Bao, J.; Qu, C., Effect of Nano-$CaCO_2$ on the Mechanical Properties and Durability of Concrete Incorporating Fly Ash., *Advances in Materials Science and Engineering*, **2020**, 7365862.
13. Meng, T.; Yu, Y.; Wang, Z., Effect of nano-$CaCO_3$ slurry on the mechanical properties and micro-structure of concrete with and without fly ash., *Composites Part B: Engineering*, **2017**, 117, 124–129.
14. Ariyagounder, J.; Veerasamy, S., Experimental Investigation on the Strength, Durability and Corrosion Properties of Concrete by Partial Replacement of Cement with Nano-SiO_2, Nano-$CaCO_3$ and Nano-$Ca(OH)_2$., *Iranian Journal of Science and Technology, Transactions of Civil Engineering*, **2022**, 46, 201–222.
15. Abdalla, J. A.; Thomas, B. S.; Hawileh, R. A.; Yang, J.; Jindal, B. B.; Ariyachandra, E., Influence of nano-TiO_2, nano-Fe_2O_3, nanoclay and nano-$CaCO_3$ on the properties of cement/geopolymer concrete., *Cleaner Materials*, **2022**, 4, 100061.
16. Jayakumari, B. Y.; Swaminathan, E. N.; Partheeban, P., A review on characteristic studies on carbon nanotubes-based cement concrete., *Construction and Building Materials*, **2023**, 367, 130344.